Radiation Measurements xxx (2013) 1–10

Contents lists available at SciVerse ScienceDirect

Radiation Measurements

journal homepage: www.elsevier.com/locate/radmeas

Photon dosimetry methods outside the target volume in radiation therapy: Optically stimulated luminescence (OSL), thermoluminescence (TL) and radiophotoluminescence (RPL) dosimetry

Q3 Željka Knežević [a,*], Liliana Stolarczyk [b], Igor Bessieres [c], Jean Marc Bordy [d], Saveta Miljanić [a], Paweł Olko [b]

[a] Ruđer Bošković Institute, Bijenička 54, 10000 Zagreb, Croatia
[b] Institute of Nuclear Physics, Radzikowskiego 152, Krakow, Poland
[c] Commissariat à l'Énergie Atomique, LIST, DCSI, 91191 Gif sur Yvette, France
[d] Commissariat à l'Énergie Atomique, LIST, LNE/LNHB, 91191 Gif sur Yvette, France

HIGHLIGHTS

- Photon dosimetry methods for out-of-field dose measurements in radiation therapy.
- Thermoluminescence, optically stimulated luminescence and radiophotoluminescence.
- Characteristics and comparison of OSL, TL and RPL dosimeters.

ARTICLE INFO

Article history:
Received 16 April 2012
Received in revised form
13 December 2012
Accepted 11 March 2013

Keywords:
Photon dosimetry methods
Thermoluminescent dosimeters (TLD)
Optically stimulated dosimeters (OSLD)
Radiophotoluminescent dosimeters (RPL)
Out-of-field dosimetry in radiation therapy

ABSTRACT

Dosimetry methods outside the target volume are still not well established in radiotherapy. Luminescence detectors due to their small dimensions, very good sensitivity, well known dose and energy response are considered as an interesting approach in verification of doses outside the treated region. The physical processes of thermoluminescence (TL), radiophotoluminescence (RPL) and optically stimulated luminescence (OSL) are very similar and can be described in terms of the energy band model of electron-hole production following irradiation.

This work is a review of the main dosimetric characteristics of luminescence detectors which were used in experiments performed by EURADOS Working Group 9 for in-phantom measurements of secondary radiation (scattered and leakage photons). TL LiF:Mg,Ti detectors type MTS-7 (IFJ PAN, Poland), types TLD-100 and TLD-700 (Harshaw), OSL Al_2O_3:C detectors type nanoDot™ (Landauer Inc.) and RPL rod glass elements type GD-352M (Asahi Techno Glass Coorporation) are described. The main characteristics are discussed, together with the readout and calibration procedures which lead to a determination of absorbed dose to water.

All dosimeter types used show very good uniformity, batch reproducibility and homogeneity. For improved accuracy, individual sensitivity correction factors should be applied for TL and OSL dosimeters while for RPL dosimeters there is no need for individual sensitivity corrections.

The dose response of all dosimeters is linear for a wide range of doses.

The energy response of GD-352M type dosimeters (with Sn filter) used for out-of-field measurements is flat for medium and low energy X-rays.

The energy dependence for TLDs is low across the range of photon energies used and the energy correction was neglected. A significant over response of Al_2O_3:C OSLDs irradiated in kilovoltage photon beams was taken into account. The energy correction factor f_{en} was calculated by using the 2006 PENELOPE Monte Carlo code.

With suitable calibration, all dosimeter types are appropriate for out-of-field dose measurements as well as for the in-phantom measurements of radiotherapy MV X-rays beams.

* Corresponding author. Tel.: +385 1 4561098; fax: +385 1 4680098.
E-mail addresses: zknezevi@gmail.com, zknez@irb.hr (Ž. Knežević).

1350-4487/$ – see front matter © 2013 Published by Elsevier Ltd.
http://dx.doi.org/10.1016/j.radmeas.2013.03.004

1. Introduction

The goal of rapidly evolving radiation treatment technologies such as intensity-modulated radiotherapy (IMRT) or tomotherapy is improvement in local tumor control. The priority during treatment planning is to apply the maximum dose to the tumor whilst minimizing side effects, such as normal tissue complications. It has been recognized for some time that irradiation of healthy tissues with low doses of scattered radiation from patient and machine collimator, leakage photons and secondary neutrons may increase the risk of development of secondary cancers remotely from the target volume (Newhauser and Durante, 2011). Growing interest in the dosimetry of out-of-field doses (sometimes referred to as peripheral doses) has resulted in a number of in-phantom measurements (Xu et al., 2008), for which passive solid state detectors, such as thermoluminescence detectors (TLDs), detectors based on optically stimulated luminescence (OSLDs) and radiophotoluminescence (RPL) glasses, may be suitable. TL, OSL and RPL dosimeters are reusable and provide stand-alone measurement techniques (i.e. they do not need cables or other physical connectors). Usually during measurements performed distantly from the target volume, doses are smaller than 1 Gy and correction for nonlinear dose response of TL, OSL and RPL detectors is not necessary. The energy dependence of dosimeters in the experiments, where the effective energy of the photon radiation field is difficult to assess, is important and will be analyzed for all three types of dosimeters.

This paper presents a brief overview of the properties of TL (MTS-7, TLD-100, TLD-700), OSL (nanoDot™) and RPL (GD-352M) dosimeters, which were used by EURADOS Working Group 9 (WG 9) for in-phantom measurements of out-of-field doses from scattered photons for modern radiotherapy techniques. Results and description of experiments performed by WG 9 are provided (Bordy et al., in this issue) and (Miljanić et al., in this issue).

2. Basic principles of thermoluminescence (TL), optically stimulated luminescence (OSL) and radiophotoluminescence (RPL)

The basic principles of thermoluminescence (TL), optically stimulated luminescence (OSL) and radiophotoluminescence (RPL) are described in Fig. 1 in terms of the energy band model of electron-hole production following irradiation.

TL and OSL are processes in which light is emitted from an irradiated insulator or semiconductor during exposure to heat (TL) or light of a specific wavelength (OSL). The TL and OSL intensity is a function of absorbed dose in a sample and thus can be used as a basis of radiation dosimetry methods. The process begins with irradiation causing ionization of valence electrons and creation of electron-hole pairs. Pre-existing defects within the material localize the free electrons and holes through non-radiative transitions. Subsequent heating or illumination with light of the irradiated sample leads to the absorption of energy by trapped electrons and transitions from the localized trap into the conduction band. Recombination of the freed electrons with the localized holes results in radiative emission and luminescence i.e. the stored energy is released in the form of visible light (the TL or OSL signal is proportional to the dose). It is not clear that the same defect centers are involved in both TL and OSL processes in any material (Bøtter-Jensen et al., 2003).

The RPL dosimeter consists of silver activated phosphate glass. The silver atoms doped in the phosphate glass exist uniformly and stably in the form of Ag^+ ions. When the phosphate glass is exposed to ionizing radiation, electrons are lifted up into the conduction band, trapped by silver ions and form stable RPL luminescent centers (Ag^0). RPL centers can occur also by the migration of holes through glass and combine with Ag^+ ions to form Ag^{++}. This mechanism is presented in the following reactions (ATGC, 2007):

$$PO_4 - e^- = hPO_4$$

$$Ag^+ + e^- = Ag^0(\text{electron trap})$$

$$Ag^+ + hPO_4 = Ag^{++}(\text{hole trap})$$

RPL centers (Ag^0 and Ag^{++}) excited with the UV light release an orange luminescence of intensity proportional to absorbed dose. Ag^0 and Ag^{++} centers do not return to the Ag^+ state until the temperature is raised to the annealing conditions. This enables the possibility of multiple readout of RPL detectors without destroying the signal, which differentiates RPL from TL and OSL.

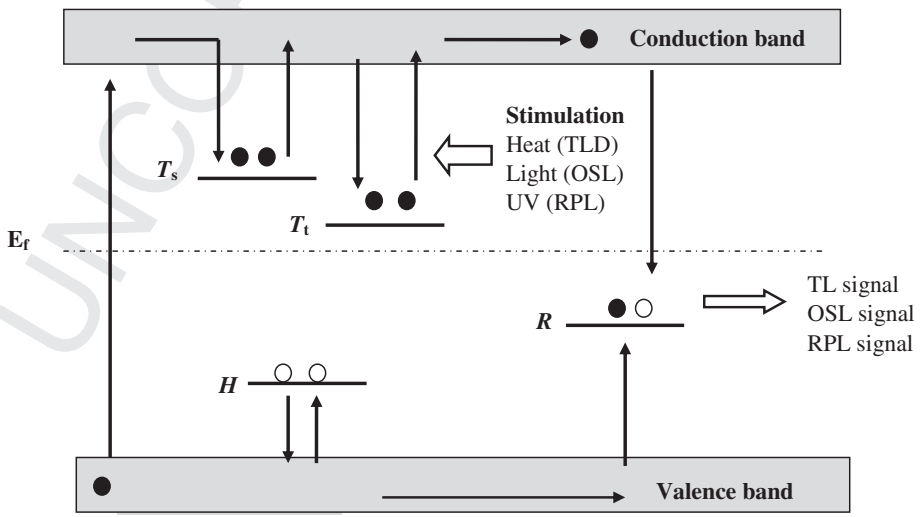

Fig. 1. Basic principles of TL, OSL and RPL process. Ionizing radiation creates electron-hole pairs. These electrons and holes become trapped at defects *T* and *H*. The trap T_s represents an unstable trap, from where the probability of escaping is large. T_t is a trap for storage of electrons where the probability of escaping (without external stimulation) is negligible. By stimulating the sample either thermally (TL), optically (OSL) or by UV (RPL), electrons gain sufficient energy to escape from trap and recombine with holes in recombination centres (*R*). The recombination is followed by the emission of light. E_f is the Fermi level.

Please cite this article in press as: Knežević, Ž., et al., Photon dosimetry methods outside the target volume in radiation therapy: Optically stimulated luminescence (OSL), thermoluminescence (TL) and radiophotoluminescence (RPL) dosimetry, Radiation Measurements (2013), http://dx.doi.org/10.1016/j.radmeas.2013.03.004

3. Luminescence dosimeters for out-of-field dosimetry in radiotherapy

In medicine, radiobiology and especially in modern radiotherapy, small size luminescence dosimeters (TL and OSL dosimeters) are applied for validation of radiotherapy treatment planning systems (Waligórski et al., 2002), for verification of treatment plans in anthropomorphic phantoms (Al-Hallaq et al., 2006; Han et al., 2008) and for in vivo (Costa et al., 2010) and two-dimensional (2-D) (Olko et al., 2008) dosimetry. TLDs find their application as transfer dosimeters during quality audits of the dose delivered by radiotherapy treatment machines (Izewska et al., 2002). An overview of dosimetry measurements in radiotherapy (in primary beams) with RPL detectors type GD-301 and GD-302M is shown in Table 1 in chronological order. A very interesting area of experiments with luminescence detectors is dosimetry of out-of-field doses. These doses received by patients were investigated for different radiation therapeutic modalities, different types of radiation and different tumor localizations. Table 2 chronologically summarizes recently published dosimetry studies on peripheral doses in radiotherapy performed with TL and OSL dosimeters.

In experiments performed by WG 9 (Bordy et al., in this issue; Miljanić et al., in this issue) three types of TL LiF:Mg,Ti detectors: MTS-7, TLD-100 and TLD-700, were used. WG 9 used also OSL Al_2O_3:C nanoDot™ detectors and RPL detectors type GD-352M. Basic characteristics of the above detectors are presented in Table 3 and Table 4.

The most fundamental feature of LiF:Mg,Ti (MTS-7, TLD-100 and TLD-700) detectors is that they are based on a lithium fluoride matrix with magnesium defects. The range of dopant concentrations for LiF:Mg,Ti is usually reported to vary between 0.01 and 0.02% for Mg and 10–15 ppm for Ti (Bilski, 2002). LiF detectors with effective atomic number $Z_{eff} = 8.14$ are considered as tissue equivalent (McKeever, 1985). For TL detectors sensitivity correction is a commonly used technique of improving the accuracy of measurements (Table 4). The stability of the TL system may be even within 2% (Toivonen, 1993), but may depend on TL reader quality and stability and also on dosimeter type and type of radiation (Oliveira and Caldas, 2004).

The nanoDot™ (Landauer Inc.) dosimeters contain a single circular OSL dosimeter (5.0 mm in diameter) placed in an adapter. The sensitive diameter of the detector is 5 mm and an effective depth of 0.1 g/cm^2 is assumed as the point of measurement. An excellent review of OSL systems was published by Akselrod et al. (2007). NanoDot™ OSL dosimeters show good uniformity in sensitivity, as the Al_2O_3:C powder used in their production is a homogenized mixture of different crystals. To improve the accuracy, in measurements performed by WG 9, sensitivity correction factors for particular dosimeters were applied. Their values varied between 91% and 107% and were given by the manufacturer. The nanoDot™ OSLDs cannot be annealed to high temperatures, as in the case of the single crystals, because of the plastic holder. Although the OSL signal can still be erased by optical illumination (bleaching), sensitivity changes related to filling of deep traps in the crystal cannot be reversed (McKeever and Moscovitch, 2003). Jursinic (2007) observed that the sensitivity is unchanged up to accumulated doses of 20 Gy, but decreases for higher doses.

RPL dosimeters that are most commonly used in the field of medical dosimetry are small glass rods (GD-300 series). The weight composition of RPL glass is as follows: 31.55% P, 51.16% O, 6.12% Al, 11.0% Na, 0.17% Ag (Piesch, 1972). The effective atomic number and density are 12.04 and 2.61 g/cm^3 respectively. The active dose readout volume is 1 mm in diameter and 0.6 mm depth located 0.7 mm from the end of the rod. The GD type RPL dosimeter has a plastic holder with holder cap with walls of 0.3 mm thickness. The geometrical readout center of GD type RPLs is 1 mm from the cap surface (ATGC, 2007). In measurement campaigns that were done by WG 9, the GD-352M type of RPL dosimeters was used. This type contains an energy compensation tin filter and is suitable for out-of-field dose measurements where scattered photons predominate. There is no need for individual sensitivity corrections because for RPL dosimeters, variability of individual response is very small (Perks et al., 2005) (Table 4).

Table 1
The overview of the experiments that used small RPL glass rod dosimeters type GD in radiotherapy.

Type of dosemeter	Type of experiment/treatment	Authors
GD-301 and GD-302M (without energy compensation filter) for use in radiotherapy		
GD-301	Measurement of absorbed dose in mice exposed to ^{137}Cs	Hoshi et al. (2000)
GD-301	Dosimetric characteristics for 4, 6 and 18 MV X-rays (water phatnom)	Tsuda (2000)
GD-301	Measurements of Gamma Knife helmet output factors	Araki et al. (2003)
GD-302M	Dose measurements on patients and physicians during endovascular brain treatment	Nishizawa et al. (2003)
GD-301	Dosimetric properties in high energy photon beams from alinac (4 and 10 MV) and Cyberknife (6 MV)	Araki et al. (2004)
GD-301	In vivo dose measurements on head and neck cancer patients during high dose brachytherapy	Nose et al. (2005)
GD-302M	Stereotactic radiosurgery dosimetric audit	Perks et al. (2005)
GD-302M	Measurement of internal dose distribution of ^{90}Y beta-ray source in a phantom simulated mice	Sato et al. (2006)
GD-302M	Study of dosimetric characteristics for X-ray ^{137}Cs and ^{60}Co irradiation	Hsu et al. (2007)
GD-301	Comparison of RPL and TLD characteristics in the field of ^{137}Cs and ^{60}Co source	Zhuo et al. (2007)
GD-302M	In vivo HDR brachytherapy phantom dose measurements	Hsu et al. (2008)
GD-302M	Comparison of RPL and TLD for postal dosimetry audit for high energy photon beams (^{60}Co, X-rays from a linac: 4, 6, 10, 20 MV)	Mizuno et al. (2008)
GD-302M	Measurement of entrance surface doses on patients and physicians during uterine artery embolisation and organ and tissue dose measurement with RPL and TLD	Nishizawa et al. (2008)
GD-301	In vivo dosimetry study for HDR interstitial brachytherapy for patients with pelvic malignancy	Nose et al. (2008)
GD-301	Measurement of output factors for CyberKnife (6 MV linac)	Rah et al. (2008)
GD-301	Study of dosimetric characteristics for use in QA audit program (in ^{60}Co beam, photon beams from linac 6, 15 MV and electron beams 6–20 MeV)	Rah et al. (2009)
GD-301	Postal dosimetry audit for high-energy photon beams (^{60}Co, photon beams from linac, 6, 10,15 MV)	Rah et al. (2009a)
GD-301	Dosimetric characteristics for total body irradiation (TBI) treatment and in vivo dose measurements on TBI patients	Rah et al. (2011)
GD-302M	Measurements of output factors for Gamma Knife for different helmet collimators	Hsu et al. (2011)
GD-302M	Dosimetric characteristics in high energy photon (4, 6, 10, 15 MV) and electron beams (5, 7, 8, 9, 10, 12, 16, 20 MeV)	Son et al. (2011)

Note: Size of the glass element of GD-301type is $\Phi 1.5 \times 8.5$ mm^2 and of GD-302M type is $\Phi 1.5 \times 12$ mm^2.

Please cite this article in press as: Knežević, Ž., et al., Photon dosimetry methods outside the target volume in radiation therapy: Optically stimulated luminescence (OSL), thermoluminescence (TL) and radiophotoluminescence (RPL) dosimetry, Radiation Measurements (2013), http://dx.doi.org/10.1016/j.radmeas.2013.03.004

Table 2
The overview of recently published dosimetry studies on peripheral doses performed in radiotherapy with TL and OSL dosimeters.

Type of dosemeter (TLD/OSLD)	Type of experiment/treatment	Authors
OSLD Al_2O_3:C (Luxel)	In vivo determination of extra-target doses received from serial tomotherapy	Meeks et al. (2002)
TLD CaF_2 (TLD-200)	Radiotherapy of Hodgkin's disease in early pregnancy: embryo dose measurements	Mazonakis et al. (2003)
TLD LiF:Mg,Ti (TLD-700)	Peripheral neutron and gamma doses in radiotherapy with an 18 MV linear accelerator	Vanhavere et al. (2004)
TLD LiF:Mg,Ti (TLD-600, TLD-700)	Measurements of secondary neutron dose from 15 MV to 18 MV IMRT	Howell et al. (2005)
TLD LiF:Mg,Ti (TLD-700, TLD 100)	Out-of-field photon and neutron dose equivalents from step-and-shoot intensity modulated radiation therapy	Kry et al. (2005)
TLD LiF:Mg,Ti (TLD-700)	Dose evaluation in lung-equivalent media in high-energy photon external radiotherapy	Duch et al. (2006)
TLD LiF:Mg,Ti (TLD 700, TLD 600)	In vivo and phantom measurements of the secondary photon and neutron doses for prostate patients undergoing 18 MV IMRT	Reft et al. (2006)
TLD LiF:Mg,Cu,P (GR-200A)	Dosimetric analysis of thyroid doses from total cranial irradiation	Acun et al. (2007)
TLD LiF:Mg,Cu,P (MCP-600D, MCP-700D)	Characterisation of MCP-600D and MCP-700D thermoluminescence detectors and their applicability for photoneutron detection	Brunckhorst et al. (2008)
TLD LiF:Mg,Ti (TLD-600, TLD-700)	Determination of the neutron spectra around an 18 MV medical LINAC with a passive Bonner sphere spectrometer based on gold foils and TLD pairs	Esposito et al. (2008)
TLD LiF:Mg,Ti (TLD-100)	Is electron beam intraoperative radiotherapy (ELIOT) safe in pregnant women with early breast cancer? In vivo dosimetry to assess fetal dose	Galimberti et al. (2009)
TLD LiF:Mg,Cu,P (GR-200A)	The investigation of fetal doses in mantle field irradiation	Karacam et al. (2009)
TLD LiF:Mg,Cu,P	In-Phantom peripheral organ doses from prostate irradiation using 18 MV external beam radiotherapy measured with 6LiF:Mg,Cu,P & 7LiF:Mg,Cu,P glass-Rod TLDs	Takam et al. (2009)
TLD LiF:Mg,Ti (TLD-600, TLD-700)	Neutron fluence in antiproton radiotherapy, measurements and simulations	Bassler et al. (2010)
TLD LiF:Mg,Ti (TLD-100)	Methodology for determining doses to in-field, out-of-field and partially in-field organs for late effects studies in photon radiotherapy	Howell et al. (2010a)
TLD LiF:Mg,Ti (TLD-100)	Accuracy of out-of-field dose calculations by a commercial treatment planning system	Howell et al. (2010b)
TLD LiF:Mg,Ti (TLD-600, TLD-700)	Dose estimation of the neutrons induced by the high energy medical linear accelerator using dual-TLD chips	Hsu et al. (2010)
TLD LiF:Mg,Ti (TLD-100)	Out-of-field photon dose following removal of the flattening filter from a medical accelerator	Kry et al. (2010)
TLD LiF:Mg,Ti (TLD-100)	Effect of organ size and position on out-of-field dose distributions during radiation therapy	Scarboro et al. (2010)
TLD LiF:Mg,Cu,P (MCP-N)	Organ and effective doses from verification techniques in image-guided radiotherapy	Dufek et al. (2011)
TLD LiF:Mg,Ti	The role of shielding in superficial X-ray therapy	Medvedevas et al. (2011)
TLD α-Al_2O_3 (TLD-500) and TLD LiF:Mg,Ti (TLD-700)	Explicit estimation of out-of-field neutron and gamma dose equivalents during proton therapy using thermoluminescence-dosimeters	Mukherjee et al. (2011)
TLD LiF:Mg,Ti (MTS-6, MTS-7)	Evaluation of risk of secondary cancer occurrence after proton radiotherapy of ocular tumours	Stolarczyk et al. (2011)
TLD LiF:Mg,Ti (TLD-100)	Assessing doses of radiotherapy with the risk of developing cancer in the head and neck	Yu et al. (2011)
OSLD Al_2O_3:C (microStar™ DOT), TLD LiF	Estimating dose to implantable cardioverter-defibrillator outside the treatment fields using a skin QED diode, optically stimulated luminescent dosimeters, and LiF thermoluminescent dosimeters	Chan et al. (2012)
TLD	Involved field radiation for Hodgkin's lymphoma: the actual dose to breasts in close proximity	Dabaja et al. (2012)
TLD LiF:Mg,Ti (TLD-100)	Second cancer incidence risk estimates using BEIR VII models for standard and complex external beam radiotherapy for early breast cancer	Donovan et al. (2012)
TLD LiF:Mg,Ti (TLD-600, TLD-700)	Out-of-field dose measurements in a water phantom using different radiotherapy modalities	Kaderka et al. (2012)
TLD LiF:Mg,Ti (TLD-100)	Scattered dose to radiosensitive organs and associated risk for cancer development from head and neck radiotherapy in pediatric patients	Kourinou et al. (in press)
TLD LiF:Mg,Cu,P (TLD-100H), TLD LiF:Mg,Ti (TLD-100)	Assessment of leakage doses around the treatment heads of different linear accelerators	Lonski et al. (in press)
TLD LiF:Mg,Ti (TLD-100)	Thyroid exposure to scattered radiation and associated cancer risk from pediatric radiotherapy for extracranial tumors	Mazonakis et al. (in press)
OSLD Al_2O_3:C (nanoDots)	Energy response of optically stimulated luminescent dosimeters for non-reference measurement locations in a 6 MV photon beam	Scarboro et al. (2012)

4. Principles of readout, annealing and measurement procedure of TL, OSL and RPL dosimeters

Dosimetry with TLDs requires complex thermal annealing steps (Table 5), which result in re-establishing the defect equilibrium. High precision is required for the stability and accuracy of the time–temperature profile of the annealing procedure because changes of the order of a few degrees can lead to significant changes in the charge migration and the sensitivity of TLDs (McKeever and Moscovitch, 2003). The main emission band of the

Table 3
Characteristic of different detectors used for out of field measurements (WG 9 EURADOS).

Detector	Material	Form	Dimensions (mm)	Z_{eff}	Reader
MTS-7 (IFJ PAN, Poland)	^{7}LiF: Mg, Ti,	Pellet	Φ 4.5 × 0.9	8.14	RA'94 TL Reader-Analyser (Mikrolab, Poland)
TLD-700 (Harshaw)	^{7}LiF: Mg, Ti	Pellet	Φ 4.5 × 0.9	8.14	Modified TOLEDO 654 reader (Vinten)
TLD-100 (Harshaw)	^{nat}LiF: Mg, Ti	Pellet	Φ 4.5 × 0.9	8.14	Modified TOLEDO 654 reader (Vinten)
nanoDot™ dosimetry system (Landauer Inc.)	Al_2O_3:C	Pellet adapter	d = 5 mm 10 × 10 × 2 mm	11.28	Semiautomatic reader MicroStarTM (Landauer Inc.)
RPL (GD-352M) (ATGC)	Ag activated Phosphate glass	Rod holder	Φ 1.5 × 12 Φ 4.3 × 14.5	12.04	Automatic reader Dose Ace (FGD-1000)

Please cite this article in press as: Knežević, Ž., et al., Photon dosimetry methods outside the target volume in radiation therapy: Optically stimulated luminescence (OSL), thermoluminescence (TL) and radiophotoluminescence (RPL) dosimetry, Radiation Measurements (2013), http://dx.doi.org/10.1016/j.radmeas.2013.03.004

Table 4
The uniformity, reproducibility and fading for the TLD: MTS, TLD-100, TLD-700, OSL nanoDot™ and RPL GD-352M.

Detector	Uniformity	Reproducibility	Fading
MTS-7 (this work)	3%[a] 2%[b]	2%	<5% (per year)
TLD-700 (Miljanić et al., 2002)	3%	4%	<5% (per year)
TLD-100 (Miljanić et al., 2002)	4%	3%	<5% (per year)
OSL, NanoDot™ (Reft, 2009)	4%[b]	1%	–
RPL (GD-352M) (Knežević et al., 2011)	1.1–1.7%	0.4%	1.7% (150 days)

[a] (without sensitivity correction).
[b] (with sensitivity correction).

emission spectrum for TL from LiF:Mg,Ti detectors consists of two, overlapping Gaussian-shaped bands at 399 nm and 473 nm (Mandowska et al., 2002). The readout of MTS-7 (Table 3) was performed with the RA'94 TL Reader-Analyser reader with platinum planchet heating and an EMI bi-alkali 9789QB photomultiplier tube with BG-12 infrared filter. The readout of TLD-100 and TLD-700 dosimeters (Table 3) was carried out using a modified manual TOLEDO 654 (Vinten) reader which enables detailed analysis and integration of the glow curves with variable integration limits (Knežević et al., 2005).

The read-out of nanoDot™ (Landauer Inc.) dosimeters with a plastic adapter, which provides protection from light, was performed in the semiautomatic reader MicroStar™. NanoDot™ system (Perks et al., 2007). This uses continuous wave OSL (CW-OSL) which consists of the continuous illumination of the dosimeters while monitoring the OSL intensity in a 1 s illumination-read period (the initial OSL intensity). The optical stimulation in the MicroStar™ reader is produced using an array of 38 green LEDs operating in conjunction with a coloured glass bandpass filter producing a peak emission at 540 nm (Jursinic, 2007; Yukihara and McKeever, 2008). The OSL signal is measured by a photomultiplier tube filtered by a glass bandpasss filter (Hoya B-370) providing a peak sensitivity at 420 nm. Depending on the dose level, two light intensities are possible: for low doses, all 38 LEDs are used, resulting in maximum stimulation and higher OSL signal, but also a larger degree of signal depletion; for high doses, only 6 LEDs are used, resulting in a lower OSL signal, but a low degree of signal depletion (Jursinic, 2007; Yukihara and McKeever, 2008). For experiments carried out by WG 9 the calibration of the MicroStar™ reader was performed in air separately for low (<150 mGy) and high doses (>150 mGy). The calibration factor for low doses is 1.607×10^{-7} Gy/pulse and for high doses is 2.682×10^{-6} Gy/pulse.

Table 5
Evaluation parameters for TL (MTS-7, TLD-100, TLD-700) and RPL GD-352M dosimeters used in WG 9 measurements.

Detector	MTS-7	TLD-100 TLD-700	RPL (GD-352M)
Pre-irradiation annealing			
Temperature (°C)	400 + 100	400 + 100	400
Time (min)	60 + 120	60 + 120	20 or 60 (>1 Gy)
Preheat			
Temperature (°C)	100	100	70
Time (min)	10	20	30
Readout			
Temperature (°C)	360	270	UV excitation
Time (s)	60	35	
Heating rate (°C/s)	5	10	

The RPL dosimeter is an accumulation type solid state dosimeter. The light is emitted whenever laser pulses (20 pulses/second) excite the glass; therefore the signal can be read multiple times in a short time without destroying it and it is possible to achieve a statistically better reproducibility by averaging many readouts. The fluorescence emitted in glass by excitation by a pulsed UV laser attenuates with time (ATGC, 2007).

The dose reading of GD type RPL dosimeters is done automatically on the FDG-1000 reader. The FGD-1000 reader produces a 337.1 nm wavelength pulsed ultraviolet laser beam to excite the dosimeters which then emit a (600–700 nm) orange luminescence. Dose reading is done automatically by setting the glass elements into the readout magazine (20 elements or less). The reader is automatically calibrated using the internal calibration element and standard irradiation element (calibration is done free in air) and provides a direct measure of dose. The internal calibration glass element is calibrated annually by an external standard RPL dosimeter traceable to a secondary standards laboratory (ATGC, 2007). By using a reference glass rod dosimeter (standard irradiation element) simultaneously with a sample dosimeter, a smaller standard deviation of dose measurements in comparison to some other dosimetry techniques (Araki et al., 2003) can be achieved. In order to eliminate stable RPL centers which are created by irradiation, the dosimeters should be annealed. Additionally after irradiation and before readout the RPL dosimeters should be preheated in order to accelerate the build-up activity (Table 5). Build-up is a phenomenon whereby the RPL intensity increases over a period of time and eventually stabilizes (up to one month to fully stabilize as reported by manufacturer). Build-up can be accelerated to saturation by a preheating process (ATGC, 2007).

5. Calibration procedure of TL, OSL and RPL dosimeters during EURADOS WG 9 experiments

Absorbed dose to water D_w is the quantity of main interest in radiation therapy, since it is well defined and water is nearly tissue equivalent for photons (TRS No. 398, IAEA, Vienna, 2000). However, irradiation of passive solid state detectors directly in terms of D_w requires special waterproof holders, appropriate water phantoms and is more time consuming, than calibration in air. During WG 9 experiments, two approaches to calibration of TL, OSL and RPL detectors in terms of D_w, which are easy to realize and do not require specially designed equipment, were applied. In the first approach, the calibration was performed in terms of kerma free in air, K_{air} followed by the application of f_{calib}, a conversion factor from K_{air} to D_w. In the second approach, the entire calibration was performed in a phantom made of PMMA, which is considered as water-equivalent. Calibration conditions for TL, OSL and RPL dosimeters are presented in Table 6.

5.1. Calibration in terms of kerma in air, K_{air}

For the measurements of the out-of-field doses in radiotherapy, TL dosimeters types TLD-100 and TLD-700 and RPL dosimeters type GD-352M were calibrated in terms of K_{air}. TL and RPL reference dosimeters belonging to the same batch as sample dosimeters were calibrated against ^{60}Co (Table 6) at the Secondary Standard Dosimetry Laboratory at the Ruđer Bošković Institute (RBI) (Vekić et al., 2006).

In order to express the results of measurements in terms of absorbed dose to water D_w conversion factors f_{calib} from K_{air} to D_w were determined experimentally for TLD and RPL detectors according to following formula:

Please cite this article in press as: Knežević, Ž., et al., Photon dosimetry methods outside the target volume in radiation therapy: Optically stimulated luminescence (OSL), thermoluminescence (TL) and radiophotoluminescence (RPL) dosimetry, Radiation Measurements (2013), http://dx.doi.org/10.1016/j.radmeas.2013.03.004

Table 6
Conditions of calibration of passive solid states detectors: TLD, OSLD and RPL.

Detector	MTS-7	TLD-100 TLD-700	RPL (GD-352M)	OSL nanoDot™
Calibration source	^{60}Co	^{60}Co	^{60}Co	^{60}Co
Quantity	D_w	K_{air}	K_{air}	K_{air}
Phantom	PMMA	Air	Air	Air
f_{calib} conversion factor K_{air} to D_w	–	1.099 (TLD-100) 1.102 (TLD-700)	1.120	1.11
Reference chamber	PTW 30010 Farmer	PTW TW 30013 Farmer		Primary cavity chambers
Field [cm × cm]	10 × 10	10 × 10	10 × 10	10 × 10
Source to chamber distance SCD [cm]	80	100	100	100

$$f_{calib} = \frac{M_{air}/K_{air}}{M_w/D_w} \quad (1)$$

where:

M_{air} is the mean value of the signal for dosimeter sample irradiated in air
M_w is the mean value of the signal for dosimeter sample irradiated in water.
K_{air} is the known kerma in air value
D_w is the known absorbed dose to water value.

Irradiations in water were performed according to TRS 398 Code of Practice (TRS No. 398, IAEA, Vienna, 2000) at a depth of 5 cm with a ^{60}Co source at 100 cm SCD and field size 10 × 10 cm^2.

Once defined, f_{calib} conversion factor may be applied multiple times, when calibration is performed under the above conditions.

For measurements with OSL dosimeters, an internal calibration of the OSL MicroStar™ reader, performed in air against ^{60}Co source (Table 6) at Commissariat à l'Énergie Atomique, LIST CEA-LIST, France, was used. For OSL dosimeters, the correction factor from K_{air} to D_w was calculated using the ratio of mass energy absorption coefficients for water and air (absorption coefficients were taken from NIST data (NIST, 2008)). In this approach measurements in the water phantom are not necessary.

5.2. Calibration in PMMA phantom

TL MTS-7 dosimeters were calibrated in a PMMA phantom (30 × 30 × 15 cm^3) with a ^{60}Co source (Table 6). D_w was determined with an ionization Farmer type chamber at z_{ref} = 5 cm. However, MTS-7 dosimeters were calibrated at the depth of maximum dose, z_{max} = 0.5 cm. To determine D_w at z_{max} the central axis percentage depth-dose (PDD) data from TRS No. 398 were used (TRS No. 398, IAEA, Vienna, 2000). Discrepancies in the determination of absorbed dose due to density variations of PMMA and to the approximate nature of the procedures for scaling depths and absorbed dose from plastic to water were neglected.

6. Dose calculations and uncertainties for TL, OSL and RPL dosimeters during WG 9 experiments

Luminescence detectors allow only relative dosimetry to be performed i.e. no absolute dose measurements using the single detector are possible. The absorbed dose from measurements with TL, OSL and RPL detectors is derived by comparison with detectors irradiated with a known dose of radiation. Following Izewska et al. (2008), fading, nonlinearity of dose response and energy dependence were taken into account during dose calculations.

The absorbed doses derived from TL and OSL measurements were determined by the following formula:

$$D_w = N_{cal} \cdot M \cdot f_{fad} \cdot f_{lin} \cdot f_{en} \cdot f_{calib} \quad (2)$$

where:

M is the signal of a sample dosimeter after background subtraction
N_{cal} is the calibration coefficient relating signal to a known absorbed dose
f_{fad} is the fading correction factor
f_{lin} is the dose response non-linearity correction factor
f_{en} is the energy correction factor
f_{calib} is the conversion factor from K_{air} to D_w.

The absorbed dose measured with RPL detectors was calculated according to Eq. (3), Eq. (4) and Eq. (5)

$$D_{accum} = M_{sample} \cdot n_c \cdot H_{st}/m_{st} \quad (3)$$

$$D_{measured} = D_{accum} - D_{initial} \quad (4)$$

$$D_w = (D_{measured} - D_{control}) \cdot f_{calib} \quad (5)$$

In Eq. (3):

D_{accum} is the accumulated dose value
n_c is the reader correction factor
H_{st} is the dose value of the standard glass
m_{st} is the readout value of the standard dosimeter
M_{sample} is the readout value for the sample dosimeter.
After annealing, all RPL dosimeters should be read out in order to measure initial dose values $D_{initial}$ of glass elements (subtracted pre-dose).
D_w was calculated according to Equations (4) and (5) where f_{calib} is the correction factor from K_{air} to D_w and $D_{control}$ is the background dose.

In order to avoid correction for fading of the TL and OSL signal (for RPL dosimeters fading is negligible (Rah et al., 2009a)) calibration and sample detectors were irradiated on the same day. The nonlinearity correction factor f_{lin} was considered to be negligible for all detectors (see Section 8). For TLDs, the energy correction factor f_{en} was assumed to be insignificant. Also for RPL dosimeters, f_{en} was not applied (in RPL dosimeters type GD-352M an energy compensation filter is built-in). The energy correction factor f_{en} was found to be meaningful for OSL detectors (see Section 7).

The analysis of the uncertainty in dose calculations is based on the assumption that the factors in Equations (2)–(5) are uncorrelated. The combined relative standard uncertainty $u_c(D_w)$ for D_w determined from the TL, OSL or RPL measurements is the square root of the sum of the squared individual relative uncertainties (Kirby et al., 1992; Izewska et al., 2008). The combined uncertainty for TL detectors type MTS-7 is $u_{TLD}(D_w)$ = 2.9% for doses varying from 2 mGy to 5 Gy and $u_{TLD}(D_w)$ = 4.2% for doses below 2 mGy (Table 7). OSLDs are capable of providing dose estimates with an uncertainty of an order of 0.7–3.2%, depending on the readout equipment and methodology (Yukihara and McKeever, 2008). The total uncertainty estimated by Reft (2009) for nanoDot™ dosimeters is at a level of 4.7% for kilovoltages energies. In order to assign the uncertainty of reproducibility for RPL dosimeters, a set of five readings of each GD-352M dosimeter was taken and the standard

Please cite this article in press as: Knežević, Ž., et al., Photon dosimetry methods outside the target volume in radiation therapy: Optically stimulated luminescence (OSL), thermoluminescence (TL) and radiophotoluminescence (RPL) dosimetry, Radiation Measurements (2013), http://dx.doi.org/10.1016/j.radmeas.2013.03.004

Table 7
Relative standard uncertainties (1 SD in %) in the individual components and the combined uncertainty $u_c(D_w)$ in the determined dose for TLD (MTS-7) and RPL (GD-352M) dosimeters.

Factor	Relative standard uncertainties	
	MTS7 (this work)	GD-352M (this work)
M	~1.7% (2 mGy–5 Gy) ~3.5% (below 2 mGy)	~0.8% (1 mGy–2 Gy) ~1.9% (below 1 mGy)
N_{cal}	2.3%	1.5%
$f_{fad}\, f_{en}\, f_{lin}$	Negligible	
f_{ang}	–	1.2%
Combined standard uncertainties	~2.9% (2 mGy–5 Gy) ~4.2% (below 2 mGy)	~2.1% (1 mGy–2 Gy) ~2.7% (below 1 mGy)

deviation (SD) of the mean value of M was calculated (Table 7). In the calculation of the combined standard uncertainty for GD-352M dosimeters, the angular correction factor according to the data from the literature (Son et al., 2011) was taken into account.

7. Energy dependence

The energy dependence is particularly important when the spectra of the photon radiation fields are difficult to assess, as in case of the determination of dose to critical organs outside the radiation field in external beam radiotherapy. According to simulations performed by Edwards and Mountford (2004) the energy spectra outside the field edge show two main distinct regions: a broad peak below about 0.5 MeV and a lower amplitude region at higher energies from 0.5 MeV to up to the maximum energy. The lower energy peak is due to photons which have undergone single or multiple Compton scattering in the phantom and the higher energy component is mainly due to primary photons transmitted through the jaws of the secondary collimator. The narrow peak at 0.511 MeV is due to pair production interactions, which may occur in the components with a high atomic number. The intensity of peaks decreases with distance from the field edge because more X-rays undergo multiple scattering and absorption.

The energy dependence of dosimeters in photon beams is linked to their effective atomic number Z_{eff} and the probability of photon interactions. Z_{eff} values for detectors used in this work are shown in Table 3. Z_{eff} of air is equal to 7.78, of water to 7.51, and of muscle tissue to 7.64 (Johns and Cunningham, 1983). It is evident that the inherent energy dependence in comparison with tissue is the best for LiF TL detectors. In Fig. 2 Mobit et al., 2006 the OSLD, TLD and RPL dosimeters' energy response data are plotted at the kilovoltage and megavoltage energies. All detector materials over-respond in kilovoltage photon beams (more for those with a larger proportion of higher Z elements) due to higher interaction probabilities for the photoelectric effect (photoelectric mass cross section is proportional to approximately Z^3).

The highest over response of LiF:Mg,Ti TLDs by a factor of 1.37 was measured in a photon beam of 30 keV effective energy (Davis et al., 2003). An excellent discussion of the dependence of LiF TLD response on variations in photon energy spectra in radiotherapy was presented by Scarboro et al. (2011). For locations outside of the treatment field, the over response of TLDs was reported as up to 12%. During measurements of out-of-field doses made by EURADOS WG 9, the influence of the energy response of LiF TLDs type TLD-100, TLD-700 and MTS-7 was considered negligible and the energy correction factor f_{en} in Eq. (2) was neglected.

The increased response of OSLD Al_2O_3:C at lower energies is attributed to the increased probability of the photoelectric effect in the aluminum oxide. Reft (2009) measured the OSLD nanoDot™ response for photons as a function of energy from 125 kVp to 18 MV. For instance, the energy response factor is 3.5 for 35 keV X-rays. For

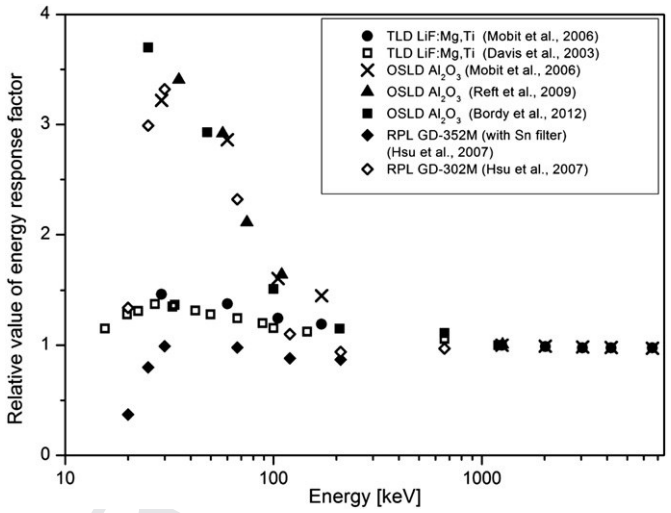

Fig. 2. The relative energy response of TLD LiF, OSLD Al_2O_3 and RPL GD-352M dosimeters for photon energies from 15 keV to 6.5 MeV normalized to ^{60}Co (TLD and OSLD) and to ^{137}Cs (RPL dosimeters).

the requirements of the dosimetry of scattered and secondary photons outside the target volume with nanoDot™ dosimeters, performed by WG 9, energy dependence was taken into account (detailed results are given in a paper provided by Bordy et al. (in this issue). f_{en} was calculated using the 2006 PENELOPE Monte Carlo code (Salvat et al., 2006). The configuration of the irradiation was simulated and the model of the entire head of the accelerator has been validated enabling precise calculations of energy fluence at each point of measurement (Fig. 3) (Bordy et al., in this issue).

Taking into account energy dependence, there are two types of glass rod RPL dosimeters: one without an energy compensation filter (GD-301 and GD-302M) and a second type containing a holder with a tin filter (GD-351 and GD-352M). Generally, the GD-301 and-GD-302M types are used in high energy photon beams in radiotherapy whereas the GD-351 and GD-352M are used in diagnostic radiology. Because RPL glasses have a relatively high density (2.61 g/cm^3) and high effective atomic number (12.04), they over-respond to low energy photons primarily due to photoelectric absorption. As shown in Fig. 2, GD-302M type (without filter) possesses very high energy dependence for low energy X-rays. Similar results were obtained with GD-301, about 350% at 30 keV (Zhuo et al., 2007). At the same time, GD-352M (with a Sn filter) shows energy dependence from −3.1% to +2.6% in the same energy range (Hsu et al., 2007). The results provided by Mizuno et al. (2008), Rah et al. (2009a), and Son et al. (2011) indicate that the RPL dosimeters GD type (without filter) are suitable for clinical and experimental use especially for in-field dose measurements in radiotherapy.

RPL dosimeters type GD-352M (with Sn filter) used for the measurements of out-of-field doses in high energy photon beams in radiotherapy performed by WG 9 showed good agreement with ionisation chamber measurements in the out-of-field region. For dose measurements at the target volume in the high energy photon field, the reading of RPL dosimeter type GD-352M overestimates the dose and should be corrected. (Bordy et al., in this issue; Miljanić et al., in this issue). In the high energy photon field, RPL glasses types GD-301 and GD-302M (without a Sn filter), should be used (Mizuno et al., 2008; Rah et al., 2009a).

8. Dose dependence

For the measurement of non-target doses in radiotherapy it is important that the dosimeters exhibit a large range of linearity

Please cite this article in press as: Knežević, Ž., et al., Photon dosimetry methods outside the target volume in radiation therapy: Optically stimulated luminescence (OSL), thermoluminescence (TL) and radiophotoluminescence (RPL) dosimetry, Radiation Measurements (2013), http://dx.doi.org/10.1016/j.radmeas.2013.03.004

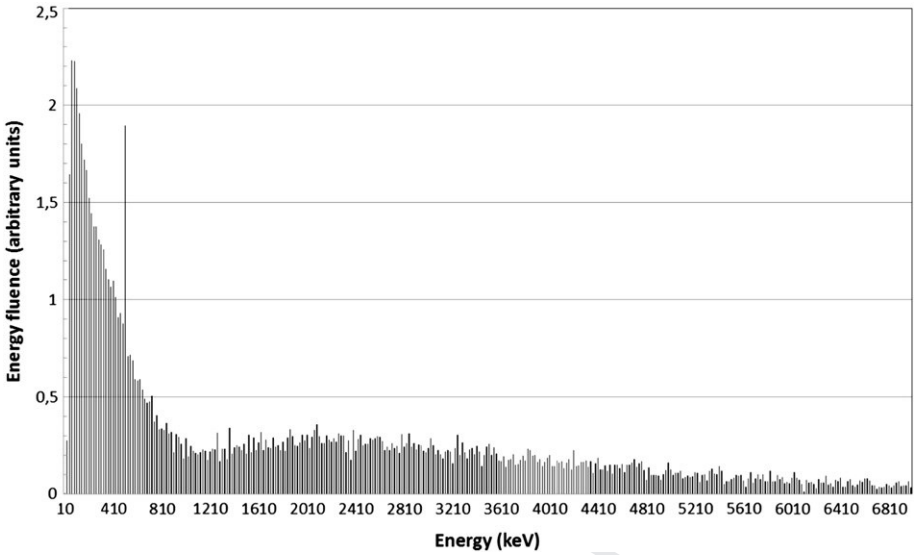

Fig. 3. Energy fluence at a measurement point at distance 18 cm from the beam axis in a water tank. Simulation was done for 12 MV X-rays with a 10 × 10 cm^2 field with a Saturne 43 at 100 cm from the source.

from low doses (~0.1 mGy) up to radiotherapy doses of a few Gy (~2 Gy).

The dose response of LiF TLDs depends on impurity composition, ionization density, supralinearity of individual glow peaks, emission spectrum, grain size, physical state, heating rate and annealing parameters (Horowitz, 1981). LiF:Mg,Ti detectors exhibit good linearity up to 2 Gy and supralinearity at higher doses (Gamboa-deBuen et al., 1998; Waligórski et al., 1999). Massillon et al. (2006) investigated the response of LiF:Mg,Ti (TLD-100) induced by ^{60}Co irradiation at doses from 4.18 mGy to 8.32 kGy. The response of the main dosimetry peaks (4 and 5) as a function of dose is linear up to ≈1Gy and supralinear for higher doses.

The OSLD dose response depends on experimental parameters: crystal growth (Yukihara et al., 2004), the optical filters used in front of the PMT (Yukihara and McKeever, 2006), the stimulation intensities (initial OSL intensity or total OSL signal) (Yukihara and McKeever, 2008) and the dose history of the dosimeter (Edmund et al., 2006). Yukihara et al. (2007) reported supralinearity for doses above 5 Gy for Luxel™ dosimeters read using a Risø TL/OSL reader. The dose response of nanoDot™ OSL dosimeters is linear up to 2 Gy with supralinearity occurring at higher absorbed doses (Reft, 2009). In general, supralinearity of OSL Al_2O_3:C dosimeters for doses above around 2 Gy was noticed (Jursinic, 2007; Schembri and Heijmen, 2007).

The response of RPL dosimeters has a good linear relationship when compared with the ion chamber response for dose ranging from 0.5 to 30 Gy. The differences were within ±2% (Araki et al., 2004). Also in the low dose range from 0.1 mGy to 500 mGy RPL dosimeters showed linear dose response with coefficient of variation 0.6–4.8% (Knezevic et al., 2011). In comparison to TL and OSL dosimeters, RPL dosimeters did not show an over-response for the higher doses.

9. Conclusions

The TL (type TLD-100, TLD-700 and MTS-7), OSL (type nanoDot™) and RPL (GD-352M) dosimeters proved to be suitable dosimetry systems for photon measurements in different clinical situations and radiotherapy treatment protocols. All types of dosimeters showed good reproducibility and uniformity. For better accuracy, individual sensitivity correction factors for TL and OSL dosimeters are used, while for RPL there is no need for individual sensitivity determination. The dose response is linear over a wide range of doses needed for out-of-field dose measurements in radiotherapy and all the dosimeters can be used down to very low doses.

TLD-100, TLD-700 and MTS-7 show very good energy dependence across all ranges of energy spectra used. For OSL nanoDot™ detectors the correction protocol has been established due to over response at low energies. Although RPL dosimeter type GD-352M shows very good agreement with ionization chamber measurements in the out-of-field region where scattered radiation prevails, at the target volume in the high energy photon field, this type overestimates dose to an extent depending on radiation energy and should be corrected (Bordy et al., in this issue). According to literature data (Rah et al., 2009; Mizuno et al., 2008) types GD-301 and GD-302M (without Sn filter) do not show energy dependence in high energy photon fields and are recommended for future measurements in the target volume. With suitable calibration, TL (type TLD-100, TLD-700 and MTS-7), OSL (type nanoDot™) and RPL (GD-352M) dosimeters are appropriate for the out-of-field dose measurements as well as for the in- or out-of- phantom dose measurements in MV X-rays beams.

Acknowledgements

This work is partly supported by the funds of the National Science Centre granted on the basis of a decision No. DEC-2011/01/N/NZ7/04657.

References

Acun, H., Kemikler, G., Karadeniz, A., 2007. Dosimetric analysis of thyroid doses from total cranial irradiation. Radiat. Prot. Dosim. 123, 498–504.

Akselrod, M.S., Botter-Jensen, L., McKeever, S.W.S., 2007. Optically stimulated luminescence and its use in medical dosimetry. Radiat. Meas. 41, S78–S99.

Al-Hallaq, H.A., Reft, C.S., Roeske, J.C., 2006. The dosimetric effects of tissue heterogeneities in intensity-modulated radiation therapy (IMRT) of the head and neck. Phys. Med. Biol. 51, 1145.

Araki, F., Ikegami, T., Ishidoya, T., Kubo, H.D., 2003. Measurements of Gamma-Knife helmet output factors using a radiophotoluminescent glass rod dosimeter and diode detector. Med. Phys. 30, 1976–1981.

Araki, F., Moribe, N., Shimonobou, T., Yamashita, Y., 2004. Dosimetric properties of radiophotoluminescent glass detector in high energy photon beams from a linear accelerator and Cyber-Knife. Med. Phys. 31, 1980–1986.

Please cite this article in press as: Knežević, Ž., et al., Photon dosimetry methods outside the target volume in radiation therapy: Optically stimulated luminescence (OSL), thermoluminescence (TL) and radiophotoluminescence (RPL) dosimetry, Radiation Measurements (2013), http://dx.doi.org/10.1016/j.radmeas.2013.03.004

ATGC, 2007. Explanation Material of RPL Glass Dosimeter: Small Element System. Asahi Techno Glass Corporation, Tokyo, Japan.

Bassler, N., Holzscheiter, M.H., Petersen, J.B., 2010. Neutron fluence in antiproton radiotherapy, measurements and simulations. Acta Oncol. 49, 1149–1159.

Bilski, P., 2002. Lithium fluoride: from LiF: Mg, Ti to LiF: Mg, Cu. P. Radiat. Prot. Dosim. 100, 199–206.

Bordy, J.M., d'Agostino, E., Bessieres, I., Domingo, C., d'Errico, F., di Fulvio, A., Knežević, Ž., Miljanić, S., Olko, P., Ostrosky, A., Poumarede, B., Sorel, S., Stolarczyk, L., Vermesse, D., Harrison, R. Out-of-field dosimetry: experimental and computational results for photons and neutrons in a water tank. Radiat. Measur., in this issue.

Bøtter-Jensen, L., McKeever, S.W.S., Wintle, A.G., 2003. Optically Stimulated Luminescence Dosimetry. Elsevier Science B.V.

Brunckhorst, E., Sheng, X., Todorovic, M., Becker, J., Cremers, F., 2008. Characterisation of MCP-600D and MCP-700D thermoluminescence detectors and their applicability for photoneutron detection. Radiat. Prot. Dosim. 131, 513–520.

Chan, M.F., Song, Y., Dauer, L.T., Li, J., Huang, D., Burman, C., 2012. Estimating dose to implantable cardioverter-defibrillator outside the treatment fields using a skin QED diode, optically stimulated luminescent dosimeters, and LiF thermoluminescent dosimeters. Med. Dosim. 37, 334–338.

Costa, A., Barbi, G., Bertucci, E., Ferreira, H., Sansavino, S., Colenci, B., Caldas, L., 2010. In vivo dosimetry with thermo luminescent dosimeters in external photon beam radiotherapy. App. Radiat. Isotop. 68, 760–762.

Dabaja, B., Wang, Z., Stovall, M., Baker, J.S., Smith, S.A., Khan, M., Ballas, L., Salehpour, M.R., 2012. Involved field radiation for Hodgkin's lymphoma: the actual dose to breasts in close proximity. Med. Dosim. 37, 374–382.

Davis, S., Ross, C., Mobit, P., Van der Zwan, L., Chase, W., Shortt, K., 2003. The response of LiF thermoluminescence dosimeters to photon beams in energy range from 30 keV X- rays to 60Co gamma rays. Radiat. Prot. Dosim. 106, 33–43.

Donovan, E.M., James, H., Bonora, M., Yarnold, J.R., Evans, P.M., 2012. Second cancer incidence risk estimates using BEIR VII models for standard and complex external beam radiotherapy for early breast cancer. Med. Phys. 39, 5814–5824.

Duch, M.A., Carrasco, P., Ginjaume, M., Jornet, N., Ortega, X., Ribas, M., 2006. Dose evaluation in lung-equivalent media in high-energy photon external radiotherapy. Radiat. Prot. Dosim. 120, 43–47.

Dufek, V., Horakova, I., Novak, L., 2011. Organ and effective doses from verification techniques in image-guided radiotherapy. Radiat. Prot. Dosim. 147, 277–280.

Edmund, J., Andersen, C., Marckmann, C., Aznar, M., Akselrod, M., Bøtter-Jensen, L., 2006. CW-OSL measurement protocols using optical fibre Al2O3:C dosimeters. Radiat. Prot. Dosim. 119, 368–374.

Edwards, C., Mountford, P., 2004. Near surface photon energy spectra outside a 6 MV field edge. Phys. Med. Biol. 49, N293–N301.

Esposito, A., Bedogni, R., Lembo, L., Morelli, M., 2008. Determination of the neutron spectra around an 18 MV medical LINAC with a passive Bonnier sphere spectrometer based on goldfoils and TLD pairs. Radiat. Meas. 43, 1038–1043.

Galimberti, V., Ciocca, M., Leonardi, M.C., Zanagnolo, V., Paola, B., Manuela, S., Sahium, R.C., Lazzari, R., Gentilini, O., Peccatori, F., Veronesi, U., Orecchia, R., 2009. Is electron beam intraoperative radiotherapy (ELIOT) safe in pregnant women with early breast cancer? In vivo dosimetry to assess fetal dose. Ann. Surg. Oncol. 16, 100–105.

Gamboa-deBuen, I., Buenfil, A., Ruiz, C., Rodríguez-Villafuerte, M., Flores, A., Brandan, M., 1998. Thermoluminescent response and relative efficiency of TLD-100 exposed to low-energy x-rays. Phys. Med. Biol. 43, 2073–2083.

Han, Y., Shin, E., Lim, C., Kang, S., Park, S., Lah, J., Suh, T., Yoon, M., Lee, S., Cho, S., Ibbott, G., Ju, S., Ahn, Y., 2008. Dosimetry in an IMRT phantom designed for a remote monitoring program. Med. Phys. 35, 2519–2527.

Horowitz, Y.S., 1981. The theoretical and microdosimetric basis of thermoluminescence and applications to dosimetry. Phys. Med. Biol. 26 (4), 765–824.

Hoshi, Y., Nomura, T., Oda, T., Iwasaki, T., Fujita, K., Ishikawa, T., Kato, A., Ikegami, T., Sakai, K., Tanooka, H., Yamada, T., 2000. Application of a newly developed photoluminescence glass dosimeter for measuring the absorbed dose in individual mice exposed to low-dose rate ^{137}Cs y-rays. J. Radiat. Res. 41, 129–137.

Howell, R.M., Ferenci, M.S., Hertel, N.E., Fullerton, G.D., Fox, T., Davis, L.W., 2005. Measurements of secondary neutron dose from 15 MV and 18 MV IMRT. Radiat. Prot. Dosim. 115, 508–512.

Howell, R.M., Scarboro, S.B., Taddei, P.J., Krishnan, S., Kry, S.F., Newhauser, W.D., 2010a. Methodology for determining doses to in-field, out-of-field and partially in-field organs for late effects studies in photon radiotherapy. Phys. Med. Biol. 55, 7009–7023.

Howell, R.M., Scarboro, S.B., Kry, S.F., Saldo, D.Z., 2010b. Accuracy of out-of-field dose calculations by a commercial treatment planning system. Phys. Med. Biol. 55, 6999–7008.

Hsu, S.-H., Yang, H.-W., Yeh, T.-C., Hsu, W.-L., Wu, C.-H., Lu, C.-C., Chen, W.-L., Huang, D.Y.C., 2007. Synthesis and physical characteristics of radiophotoluminescent dosimeters. Radiat. Meas. 42, 621–624.

Hsu, S.-H., Yeh, C.-Y., Yeh, T.-C., Hing, J.-H., Tipton, A.Y.H., Chen, W.-L., Sun, S.-S., Huang, D.Y.C., 2008. Clinical application of radiophotoluminescent glass dosimeter for dose verification of prostate HDR procedure. Med. Phys. 35, 5558–5564.

Hsu, F.-Y., Chang, Y.-L., Liu, M.-T., Huang, S.-S., Yu, Ch.-Ch, 2010. Dose estimation of the neutrons induced by the high energy medical lineal accelerator using dual-TLD chips. Radiat. Meas. 45, 739–741.

Hsu, S.-M., Lee, J.-H., Hsu, F.-Y., Lee, H.-W., Hing, S.-K., Liao, Y.-J., Lee, M.-S., 2011. Dose measurements for gamma knife with radiophotoluminescent glass dosimeter and radiochromic film. Radiat. Prot. Dosim. 146, 256–259.

Izewska, J., Bera, P., Vatnitsky, S., 2002. IAEA/WHO TLD postal dose audit service and high precision measurements for radiotherapy level dosimetry. Radiat. Prot. Dosim. 101, 387–392.

Izewska, J., Hultqvist, M., Bera, P., 2008. Analysis of uncertainties in the IAEA/WHO TLD postal dose audit system. Radiat. Meas. 43, 959–963.

Johns, H.E., Cunningham, J.R., 1983. The Physics of Radiology, fourth ed. C C Thomas, Springfield.

Jursinic, P., 2007. Characterization of optically stimulated luminescence dosimeters, OSLDs, for clinical dosimetric measurements. Med. Phys. 34, 4594–4604.

Kaderka, R., Schardt, D., Durante, M., Berger, T., Ramm, U., Licher, J., La Tessa, C., 2012. Out-of-field dose measurements in a water phantom using different radiotherapy modalities. Phys. Med. Biol. 57, 5059–5074.

Karacam, S.C., Güralp, O.S., Oksüz, D.C., Koca, A., Cepni, I., Cepni, K., Bese, N., 2009. The investigation of fetal doses in mantle field irradiation. Radiat. Prot. Dosim. 133, 165–170.

Kirby, T., Hanson, W., Johnston, D., 1992. Uncertainty analysis of absorbed dose calculations from thermoluminescence dosimeters. Med. Phys. 19, 1427–1433.

Knežević, Ž., Krpan, K., Ranogajec-Komor, M., Miljanić, S., Vekić, B., Rupnik, Z., 2005. Interface and software development for thermoluminescent dosimetry. In: Garaj Vrhovac, V., Kopjar, N., Miljanić, S. (Eds.), Proc. of 6th Symposium of the Croatian Radiation Protection Association (CRPA), Stubičke Toplice, Croatia, 18–20. 04. 2005. CRPA, Zagreb, Croatia, pp. 111–116.

Knežević, Ž., Beck, N., Milković, Đ., Miljanić, S., Ranogajec-Komor, M., 2011. Characterisation of RPL and TL dosimetry systems and comparison in medical dosimetry applications. Radiat. Meas. 46, 1582–1585.

Kourinou, K.M., Mazonakis, M., Lyraraki, E., Stratakis, J., Damilakis, J. Scattered dose to radiosensitive organs and associated risk for cancer development from head and neck radiotherapy in pediatric patients. Phys. Med., in press.

Kry, S., Salehpour, M., Followill, D., Stovall, M., Kuban, D., White, R., Rosen, I., 2005. Out-of-field photon and neutron dose equivalents from step-and-shoot intensity-modulated radiation therapy. Int. J. Radiat. Oncol. Biol. Phys. 62, 1204–1216.

Kry, S.F., Vassiliev, O.N., Mohan, R., 2010. Out-of-field photon dose following removal of the flattening filter from a medical akcelerator. Phys. Med. Biol. 55, 2155–2166.

Lonski, P., Taylor, M.L., Franich, R.D., Harty, P., Kron, T. Assesment of leakage doses around the treatment heads of different linear accelerators. Radiat. Prot. Dosim., in press. (http://dx.doi.org/10.1093/rpd/ncs049).

Mandowska, E., Bilski, P., Ochab, E., Świątek, J., Mandowski, A., 2002. TL emission spectra from disserently doped LiF:Mg detectors. Radiat. Prot. Dosim. 100, 451–454.

Massillon, G., Gamboa-deBuen, I., Brandan, M., 2006. Onset of supralinear response in TLD-100 exposed to 60Co gamma-rays. J. Phys. D: Appl. Phys. 39, 262.

Mazonakis, M., Varveris, H., Fasoulaki, M., Damilakis, J., 2003. Radiotherapy of Hodgkin's disease in early pregnancy: embryo dose measurements. Radiother. Oncol. 66, 333–339.

Mazonakis, M., Kourinou, K., Lyraraki, E., Varveris, H., Damilakis, J. Thyroid exposure to scattered radiation and associated second cancer risk from paediatric radiotherapy for extracranial tumours. Radiat. Prot. Dosim. in press (http://dx.doi.org/10.1093/rpd/ncs056).

McKeever, S.W.S., 1985. Thermoluminescence of Solids. Cambridge University Press, Cambgidge.

McKeever, S.W.S., Moscovitch, M., 2003. On the advantages and disadvantages of optically stimulated luminescence dosimetry and thermoluminescence dosimetry. Radiat. Prot. Dosim. 104, 263–270.

Medvedevas, N., Adliene, D., Laurikaitiene, J., Andrejaitis, A., 2011. The role of shielding in superficial X-ray therapy. Radiat. Prot. Dosim. 147, 291–295.

Meeks, S., Paulino, A., Pennington, E., Simon, J., Skwarchuk, M., Buatti, J., 2002. In vivo determination of extra-target doses received from serial tomotherapy. Radiother. Oncol. 63, 217–222.

Miljanić, S., Ranogajec-Komor, M., Knezevic, Z., Vekic, B., 2002. Main dosimetric characteristic of some tissue-equivalent TL detectors. Radiat. Prot. Dosim. 100, 437–442.

Miljanić, S., Bessieres, I., Bordy, J.-M., d'Errico, F., di Fulvio, A., Kabat, D., Knežević, Ž., Olko, P., Stolarczyk, L., Tana, L., Harrison, R. Clinical simulations of prostate radiotherapy using BOMAB-like phantoms: results for photons. Radiat. Meas, in this issue.

Mizuno, H., Kanai, T., Kusano, Y., Ko, S., Ono, M., Fukumura, A., Abe, K., Nishizawa, K., Shimbo, M., Sakata, S., Ishikura, S., Ikeda, H., 2008. Feasibility study of glass dosimeter postal dosimetry audit of high-energy, radiotherapy photon beams. Radiot. Oncol. 85, 258–263.

Mobit, P., Agyingi, E., Sandison, G., 2006. Comparison of the energy-response factor of LiF and Al_2O_3 in radiotherapy beams. Radiat. Prot. Dosim. 119, 497–499.

Mukherjee, B., Lambert, J., Hentschel, R., Farr, J., 2011. Explicite estimation of out-of-field neutron and gamma dose equivalents during protontherapy using thermoluminescence-dosimeters. Radiat. Meas. 46, 1952–1955.

Newhauser, W., Durante, M., 2011. Assessing the risk of second malignancies after modern radiotherapy. Nat. Rev. Cancer 11, 438–448.

Nishizawa, K., Moritake, T., Matsumaru, Y., Tsuboi, K., Iwai, K., 2003. Dose measurement for patients and physicians using a glass dosimeter during endovascular treatment for brain disease. Radiat. Prot. Dosim. 107, 247–252.

Nishizawa, K., Masuda, Y., Morinaga, K., Suzuki, S., Kikuyama, S., Zoshida, T., Ohno, M., Akahane, K., Iwai, K., 2008. Surface dose measurement in patients and physicians and effective dose estimation in patients during uterine artery embolisation. Radiat. Prot. Dosim. 128 (3), 343–350.

Please cite this article in press as: Knežević, Ž., et al., Photon dosimetry methods outside the target volume in radiation therapy: Optically stimulated luminescence (OSL), thermoluminescence (TL) and radiophotoluminescence (RPL) dosimetry, Radiation Measurements (2013), http://dx.doi.org/10.1016/j.radmeas.2013.03.004

NIST, 2008. Tables of X-ray Mass Attenuation Coefficients and Mass Energy-absorption Coefficients. National Institutes of Standards and Technology. http://physics.nist.gov/PhysRefData/.

Nose, T., Koizumi, M., Yoshida, K., Nishiyama, K., Sasaki, J., Ohnishi, T., Peiffert, D., 2005. In vivo dosimetry of high dose rate brachytherapy: study on 61 Head and Neck Cancer patients using radiophotoluminescence glass dosimeter. Int. J. Radiat. Oncol. Biol. Phys. 61, 945–953.

Nose, T., Koizumi, M., Yoshida, K., Nishiyama, K., Sasaki, J., Ohnishi, T., Kozuka, T., Gomi, K., Oguchi, M., Sumida, I., Takahashi, Y., Ito, A., Yamashita, T., 2008. In vivo dosimetry of high-dose-rate interstitial brachytherapy in the pelvic region: use of a radiophotoluminescence glass dosimeter for measurements of 1004 points in 66 patients with pelvic malignancy. Int. J. Radiat. Oncol. Biol. Phys. 70 (2), 626–633.

Oliveira, M.L., Caldas, L.V.E., 2004. Performance of different thermoluminescence dosimeters in 90Sr+90Y radiation fields. Radiat. Prot. Dosim. 111, 17–20.

Olko, P., Czopyk, L., K1osowski, M., Waligorski, M.P.R., 2008. Thermoluminescence dosimetry using TL-readers equipped with CCD cameras. Radiat. Meas. 43, 864–869.

Perks, J., Gao, M., Smith, V., Skubic, S., Goetsch, S., 2005. Glass rod detectors for small field, stereotactic radiosurgery dosimetric audit. Med. Phys. 32 (3), 726–732.

Perks, C., Le Roy, G., Prugnaud, B., 2007. Introduction of the InLight monitoring mervice. Radiat. Prot. Dosim. 125, 220–223.

Piesch, E., 1972. Developments in radiophotoluminescence dosimetry. In: Attix, F.H. (Ed.), Topics in Radation Dosimetry. Accademic Press Inc., New York, pp. 461–532.

Rah, J.-E., Shin, D.O., Jang, J.S., Kim, M.C., Yoon, S.C., Suh, T.S., 2008. Application of a glass rod detector for the output factor measurement in the CyberKnife. Appl. Radiat. Isotop. 66, 1980–19858.

Rah, J.-E., Kim, S., Cheong, K.-H., Lee, J.-W., Chung, J.-B., Shin, D.-O., Suh, T.-S., 2009. Feasibility study of radiophotoluminescenct glass rod dosimeter postal dose intercomparison for high energy photon beam. Appl. Radiat. Isotop. 67, 324–328.

Rah, J.-E., Hong, J.-Y., Kim, G.-Y., Kim, Y.-L., Shin, D.-O., Suh, T.-S., 2009a. A comparison of the dosimetric characteristics of a glass rod dosimeter and a thermoluminescent dosimeter for mailed dosimeter. Radiat. Meas. 44, 18–22.

Rah, J.-E., Hwang, U.-J., Jeong, H., Lee, S.-Y., Lee, D.-H., Shin, D.-H., Yoon, M., Lee, S.B., Lee, R., Park, S.Y., 2011. Clinical Application of glass dosimeter for in vivo dose measurements of total body irradiation treatment technique. Radiat. Meas. 46, 40–45.

Reft, C.S., Runkel-Muller, R., Myrianthopoulos, L., 2006. In vivoand phantom measurements of the secondary photon and neutron doses for prostate patients undergoing MV 18 IMRT. Med. Phys. 33, 3734–3743.

Reft, C.S., 2009. The energy dependence and dose response of a commercial optically stimulated luminescent detector for kilovoltage photon, megavoltage photon, and electron, proton, and carbon beams. Med. Phys. 36, 1690–1699.

Salvat, F., Fernandez-Varea, J.M., Sempau, J., 2006. PENELOPE-2006: A Code System for Monte Carlo Simulation of Electron and Photon Transport. OECD, Barcelona, Spain, ISBN 92-64-02301-1.

Sato, Y., Yamabayashi, H., Nakamura, T., 2006. Estimation of internal dose distribution of ^{90}Y beta-ray source implanted in a small phantom simulated mice. In: Proc. of the 13th EGS Users Meeting in Japan. KEK, Tsukupa, Japan, pp. 94–100.

Scarboro, S.B., Stovall, M., White, A., Smith, S.A., Saldo, D., Kry, S.F., Howell, R.M., 2010. Effect of organ size and position on out-of-field dose distributions during radiation therapy. Phys. Med. Biol. 55, 7025.

Scarboro, S.B., Followill, D.S., Howell, R.M., Kry, S.F., 2011. Variations in photon energy spectra of a 6 MV beam and their impact on TLD response. Med. Phys. 38, 2619–2628.

Scarboro, S.B., Followill, D.S., Kerns, J.R., White, R.A., Kry, S.F., 2012. Energy response of optically stimulated luminescent dosimeters for non-reference measurement locations in a 6 MV photon beam. Phys. Med. Biol. 57, 2505–2515.

Schembri, V., Heijmen, B., 2007. Optically stimulated luminescence (OSL) of carbon-doped aluminum oxide (Al2O3:C) for film dosimetry in radiotherapy. Med. Phys. 34, 2113–2118.

Son, K., Jung, H., Shin, S.H., Lee, H.-H., Kim, M.-S., Ji, Y.H., Kim, K.B., 2011. Evaluation of the dosimetric characteristics of a radiophotoluminescent glass dosimeter for high-energy photon and electron beams in the field of radiotherapy. Radiat. Meas. 46, 1117–1122.

Stolarczyk, L., Cywicka-Jakiel, T., Horwacik, T., Olko, P., Swakon, J., Waligorski, M., 2011. Evaluation of risk of secondary cancer occurrence after proton radiotherapy of ocular tumours. Radiat. Meas. 46, 1944–1947.

Takam, R., Bezak, E., Yeoh, E., Liu, G., 2009. In-phantom Peripheral Organ Doses from Prostate Irradiation Using 18 MV External Beam Radiotherapy Measured with 6LiF: Mg, Cu, P & 7LiF: Mg, Cu, P Glass-rod TLDs. World Congress on Medical Physics and Biomedical Engineering, September 7–12, 2009, Munich, Germany, Proceedings, 557–560.

Toivonen, M., 1993. Improving the accuracy of TLD system in clinical applications. Radiat. Prot. Dosim. 47, 497–503.

TRS 398, 2000. Absorbed Dose Determination in External Beam Radiotherapy: an International Code of Practice for Dosimetry Based on Standards of Absorbed Dose to Water. IAEA, Vienna. ISSN 1011–4289.

Tsuda, M., 2000. A Few remarks on photoluminescence dosimetry with high energy X-rays. Jpn. J. Med. Phys. 20, 131–139.

Vanhavere, F., Huyskens, D., Struelens, L., 2004. Peripheral neutron and gamma doses in radiotherapy with an 18 MV linear accelerator. Radiat. Prot. Dosim. 110, 607–612.

Vekić, B., Ban, R., Miljanić, S., 2006. Secondary standard dosimetry laboratory at the Ruđer Bošković Institute, Zagreb. Arh. Hig. Rada Toksikol. 57, 189–194 (in Croatian).

Waligórski, M., Lesiak, J., Bubula, E., Byrski, E., Ryba, E., Olko, P., Bilski, P., 1999. Application of individually calibrated solid LiF: Mg, Ti (MTS-N) detectors in clinical dosimetry. Radiat. Prot. Dosim. 85, 377–380.

Waligórski, M., Bilski, P., Lesiak, J., Byrski, E., Rozwadowska-Bogusz, B., Baranczyk, R., Gora, E., Ochab, E., Olko, P., 2002. Validation of a radiotherapy treatment planning system using an anthropomorphic phantom and MTS-N thermoluminescence detectors. Radiat. Prot. Dosim. 101, 477–480.

Xu, X., Bednarz, B., Paganetti, H., 2008. A review of dosimetry studies on external-beam radiation treatment with respect to second cancer induction. Phys. Med. Biol. 53, R193–R241.

Yu, Ch.-Ch., Hsu, F.-Y., Yu, W.-H., Liu, M.-T., Huang, S.-S., 2011. Assessing doses of radiotherapy with the risk of developing cancer in the head and Neck. Radiat. Meas. 46, 1948–1951.

Yukihara, E.G., Whitley, V.H., McKeever, S.W.S., Akselrod, A.E., Akselrod, M.S., 2004. Effect of high-dose irradiation on the optically stimulated luminescence of Al_2O_3:C. Radiat. Meas. 38, 317–330.

Yukihara, E.G., McKeever, S.W.S., 2006. Spectroscopy and optically stimulated luminescence of Al_2O_3:C using time-resolved measurements. J. Appl. Phys. 100, 083512.

Yukihara, E.G., Mardirossian, G., Mirzasadeghi, M., Guduru, S., Ahmad, S., 2007. Evaluation of Al_2O_3:C optically stimulated luminescence (OSL) dosimeters for passive dosimetry of high-energy photon and electron beams in radiotherapy. Med. Phys. 35, 260–269.

Yukihara, E.G., McKeever, S.W.S., 2008. Optically stimulated luminescence (OSL) dosimetry in medicine. Phys. Med. Biol. 53, R351–R379.

Zhuo, W., Liu, W., Huang, G., Zhu, G., Ma, G., 2007. Comparison of dosimetric properies between GD-300 series of radiophotoluminescent glass detectors and GR-200 series of thermoluminescent detectors. Nucl. Sci. Tech. 18, 362–365.

Please cite this article in press as: Knežević, Ž., et al., Photon dosimetry methods outside the target volume in radiation therapy: Optically stimulated luminescence (OSL), thermoluminescence (TL) and radiophotoluminescence (RPL) dosimetry, Radiation Measurements (2013), http://dx.doi.org/10.1016/j.radmeas.2013.03.004